Lysophosphatidic Acid Receptor 6: A Prognostic Biomarker for Lung Adenocarcinoma via Correlating Immune Infiltration

Jian He (jih003@sjtu.edu.cn)
Shanghai Jiao Tong University School of Medicine https://orcid.org/0000-0002-1426-7799
Mei Meng
Shanghai Jiao Tong University School of Medicine
Hui Wang
Shanghai Jiao Tong University School of Medicine

Primary research

Keywords: LPAR6, tumor infiltration lymphocytes, prognosis, lung adenocarcinoma, biomarker

Posted Date: July 1st, 2021

DOI: https://doi.org/10.21203/rs.3.rs-653591/v1

Abstract

Background

LPAR6 is the most recently determined GPCR of LPA, and very few of study have demonstrated the performance of LPAR6 in cancers. Moreover, the relationship of LPAR6 to prognosis potential and tumor infiltration immune cells in different cancers still unclarified.

Methods

The mRNA expression of LPAR6 and its clinical characteristics were evaluated on various databases. The association between LPAR6 and immune infiltrates of various types of cancer were investigated via TIMER. IHC for LPAR6 in LUAD and LUSC tissue microarray with patients' information was detected.

Results

We constructed a systematic prognostic landscape in various types of cancer base on the mRNA expression level. We enclosed that higher LPAR6 expression level was associated with better OS in some types of malignancy. Moreover, LPAR6 significantly affects the prognostic potential of various cancers in TCGA, especially in lung cancer. Tissue microarray's results demonstrated that higher protein level of LPAR6 was correlated with better overall survival of LUAD rather than LUSC cohorts. Further research found that the underlying mechanism of this phenome might be the expression level of LPAR6 was positively associated with infiltrating statuses of devious immunocytes in LUAD rather than in LUSC, that is, LPAR6 expression potentially contributes to the activation and recruiting of CD8 + T, naive T, effector T cell and natural killer cell and inactivates Tregs, decrease T cell exhaustion and regulate T-helper cells in LUAD.

Conclusions

Our discovery implies that LPAR6 is associated with prognostic potential and immune-infiltrating levels in LUAD. These discoveries imply that LPAR6 could be a promising biomarker for indicating prognosis potential and immune infiltration level in LUAD cohorts.

1. Introduction

Lung cancer is one of the most common malignancies around the world, and metastasis is a crucial biological procedure leading to a poor prognosis [1]. It is the top one diagnosed malignancy in China and the second most common malignancy in the U.S., also the leading cause of cancer-related deaths both in China and the U.S. [2]. Scientists have made great efforts to treat various types of lung cancer, but there is still a large amount of time and effort to do. According to histopathological classification, lung cancer could be catalogued into two broad subtypes, non-small-cell lung cancer (NSCLC) and small cell lung cancer (SCLC), and the NSCLC is more prevalent [3]. Lung adenocarcinoma (LUAD) and lung squamous cell carcinoma (LUSC) are the first and the second most common subtype NSCLC respectively [4]. Surgery is the primary treatment option during the early

stages of the NSCLC, while in late stages, surgery is combined with chemotherapies, and/or radiotherapy [4]. However, despite these treatment procedures, the prognosis of the patients remains not good, also the post-treatment recurrence is the main cause of the disease, the total 5-year survival rate for all stages is only 16.6% [4].

NSCLC has been regarded as a kind of non-immunogenic disease in the past twenty years. However, more and more knowledge of tumor immune interactions has opposed this model in lung cancer and other types of malignancy. Immune-related interaction mechanisms act as a crucial role in oncogenesis and development, and immune therapy is considered a promising approach for cancer treatment [4, 5], based on this, scientists are attempting to employ the body's own immune system to fight and prevent malignancies [6]. Recently, immunotherapies, including adoptive cell transfers, monoclonal antibodies and vaccines, have become more and more applied to the clinic treatment of many types of cancers, for example, melanoma, and more recently for lung cancer [7]. During the last decade, the finding of antibodies that target the immune checkpoints has revolutionized the treatment of NSCLC, such as PD-1 and PD-L1 [8], and these two therapy approaches (PD-1 and PD-L1), has demonstrated promising anti-tumor performance in NSCLC and melanoma [9–11]. In addition, more and more research has demonstrated that TILs (tumor-infiltrating lymphocytes) play a key role in modulating the response to chemotherapy and heighten the clinical prognosis potential of various types of cancer [12, 13], such as tumor-associated macrophages (TAMs) [14–16] and tumor-infiltrating neutrophils (TINs), they also associate with the prognosis [17–20]. So, it is an essential and urgent requirement for the explanations of the immunophenotypes of tumor immune interactions and the identification of new immune therapy targets for lung cancers.

LPA is a kind of lipid that involved in the proliferation of tumor cells via its G-protein coupled (GPC) receptors [21, 22] and one of their receptors-LPAR6 is a newly identified receptor of LPA [23, 24], and it has been demonstrated to be related to many types of tumor, including prostate [25], liver [26, 27], colorectal [28, 29] and pancreatic cancer [30]. But the function of LPAR6 remains highly controversial since in colorectal cancer, the scientists found that LPAR6 might act as a tumor suppressor whereas act as a facilitator in the other types of tumors [25–27, 30, 31]. All these indicate that LPAR6 plays a key role in cancer, but the relationship between LPAR6 and tumor biology and the underlying mechanism involved is still not well understood.

Bioinformatics is an emerging procedure that supports us to make full usage of numerous high throughput data to analyze the level of specific genes in various types of cancer [31]. So in this work, we investigated the mRNA expression level of LPAR6 and the correlation with prognosis patterns of cancer patients in databases. In addition, we analyzed the correlation of LPAR6 with tumor-infiltrating immune cells (TIICs) in various tumor microenvironments via TIMER. Moreover, IHC staining for LPAR6 in two separate lung cancer cohorts with patients' information was detected to analyze the correlation of the expression of LPAR6 and the clinicopathological parameters of lung cancer.

All these discoveries shed light on the crucial role of LPAR6 in lung cancers as well as provide a potential correlation and the mechanism involved between LPAR6 and tumor-immune interactions.

2. Materials And Methods

2.1 Ethics approval

This project was permitted by Independent Ethics Committee of Shanghai Jiao Tong University School of Medicine.

2.2 Gene expression level of the LPAR6 gene analysis

The mRNA expression level of the LPAR6 in different types of cancers was investigated via Oncomine database, TIMER and GEPIA2 database [32]. The threshold in Oncomine database was as follows: *P*-value of 0.0001, fold change of 1.5, and gene ranking top 5%.

2.3 Prognosis Analysis

The association between LPAR6 expression level and survival rate in different types of cancers was investigated by the database PrognoScan and GEPIA2, which searching for relationships between gene expression level and the prognoses of patients, such as OS and DFS, across a large collection of publicly available cancer microarray datasets [33, 34]. The threshold was adjusted to a Cox *P*-value < 0.05.

2.4 Correlation Analysis

The correlation between LPAR6 expression and survival rate as well as different cancer staging in various cancers was determined by Kaplan-Meier plotter [35]. The HR with 95% confidence intervals and log-rank *P*-value were also analyzed.

2.5 Methylation analysis

UALCAN [36] could be used to investigate methylation and relative mRNA expression levels, as well as the survival of a specific target gene across several clinicopathological features, such as stages and age. The t-test was performed to compare the statistical significance between the two independent groups.

2.6 GeneMANIA analysis

GeneMANIA is identified single genes related to a set of input genes [37] to construct the LPAR6 biological network based on a set of functional association data, including coexpression, genetic and protein interaction pathways, colocalization and protein domain homology.

2.7 LinkedOmics analysis.

Thirty-two types of cancer and over ten thousand patients from TCGA were included in the LinkedOmics database [38]. LinkFinder was used to determine the differentially expressed genes (DEGs) in TCGA. LUAD and LUSC cohorts whose expression levels correlated with those of *LPAR6*. The results were investigated by using Pearson's correlation coefficient. LinkInterpreter was employed to identify the pathways and networks [39].

2.8 Immune infiltrates level and gene correlation analysis

We investigated LPAR6 expression in various types of malignancy and the association of LPAR6 expression level with the abundance of immune infiltrating, including CD4 + T cells, CD8 + T cells, B cells, macrophages, neutrophils, and DCs, via gene modules in TIMER, which is a comprehensive resource for systematic analysis of immune infiltrates across diverse types of cancer [40–43]. In addition, associations between LPAR6 expression level and marker genes of TIICs were explored via correlation modules. The marker genes of TIICs included markers of T cells (CD8+, general), B cells, TAMs (tumor association macrophages), monocytes, macrophages (M1 and M2), natural killer (NK) cells, neutrophils, dendritic cells (DCs), T-helper (Th1, Th2 and Th17) cells,

follicular helper T (Tfh) cells, Tregs, and exhausted T cells. The gene marker sets are referenced in our previous studies [44, 45]. The expression level of the genes was demonstrated by using log2 RSEM.

GEPIA2 database was employed to confirm the significantly correlated genes in-depth, which [34] is a web server with gene expression analysis based on GTEx and TCGA databases. Furthermore, GEPIA2 was employed to generate curves of OS and DFS.

2.9 Immunohistochemical staining for LPAR6 in lung cancer patient cohort tissue microarrays

Here, two tissue microarrays were constructed using formalin-fixed, paraffin-embedded (FFPE) tissue samples from LUAD (LUC1601) and LUSC (LUC1602) patients, each TMA chip containing 74 and 78 paired tumors and adjacent normal tissues were purchased from the Superbiotek Co., Ltd., (Shanghai, China) respectively. Clinicopathological data including subtype, histological grading, and tumor/nodal stage and information about patient follow-up could be retrieved from the database of the Shanghai Jiao Tong University School of Medicine.

The tissue sections underwent immunohistochemical staining using a primary antibody to LPAR6 (Thermo Fisher/ Invitrogen, USA) (Cat No. PA5-33901) at a dilution of 1: 100. Sections of the TMAs were used to investigate the protein levels of LPAR6 following the general standard IHC staining protocols.

2.10 Statistical Analysis

The statistical analysis as the our previous work. The results produced via Oncomine are exhibited as mentioned in part 2.1. The consequence of Kaplan-Meier plots, GEPIA, and PrognoScan are exhibited with HR and *p* or Cox *p*-values from a log-rank test. And the correlation coefficient of gene expression was evaluated by Spearman's correlation and *p*-values < 0.05 were considered statistically significant.

Protein level was determined by the staining intensity and the distribution of the positive cells, which were performed by two independent pathologists blinded to the clinical information of the patients as described [45].

3. Results

3.1 The expression levels of *LPAR6* in different human cancers

To study the varied mRNA expression level of *LPAR6* expression in tumor and normal tissues, the LPAR6 mRNA expression levels were analyzed using the dominant online database (Oncomine and GEPIA2). This study enclosed that the LPAR6 expression was higher in brain and CNS cancer, gastric, kidney, liver cancer,, lymphoma and pancreatic cancer compared to the normal tissues and lower expression level of LPAR6 was observed in breast, bladder, colorectal, cervical, lung, esophageal, prostate cancer and some other types of cancer compared to the adjacent normal tissues (cancer *vs.* normal) (Fig. 1A). The detail of the expression level of *LPAR6* expression in different cancer types is summarized in **Supplementary Table 1**. To evaluate LPAR6 expression level in cancers, we determined the levels of LPAR6 expression employing the RNA-Seq datasets of multiple cancer types in the Cancer Genome Atlas (TCGA). The varied expression levels between tumor and adjacent normal tissues for LPAR6 across each type of TCGA tumors is demonstrated in Fig. 1B. The expression level of

LPAR6 was significantly lower in the tumor tissue of BLCA, BRCA, COAD, HNSC, KICH, LUAD, PRAD, READ and UCEC compared with adjacent normal tissues and was significantly higher in ESCA, KIRC, KIRP, THCA compared with adjacent normal tissues (Fig. 1B). GEPIA2 generates dot plots to profile gene/isoform expression across various types of cancer and paired normal tissue samples, and each dot representing a distinct sample. The differential mRNA expression level of LPAR6 between tumor and matched TCGA normal and GTEx data across all TCGA tumors by GEPIA2 is demonstrated in Fig. 1C. LPAR6 expression was significantly higher in GBM, KIRC, LAML, LGG, PAAD, THYM and lower in ACC, ESCA, KICH, LUAD, PRAD, TGCT, UCEC and UCS compared with normal GTEx tissues. From these above, we found that the expression pattern are different in two types of lung cancers, LUAD and LUSC.

3.2 Prognostic potential of *LPAR6* across various types of cancer

We determined whether the mRNA expression level of LPAR6 was associated with the prognosis specific across cancer patient cohorts. The effects of LPAR6 expression on the various survival rates were assessed by using the PrognoScan database. The detailed relationship between the expression level of LPAR6 and prognosis potential of various cancers are listed in **Supplementary Table 2.** Notably, the expression level of LPAR6 impacts OS in breast and lung cancer significantly (Fig. 2A-M). Two cohorts (GSE3141 and GSE4573) of lung cancer demonstrated that high expression level of LPAR6 was associated with better prognosis (OS HR = 0.53, 95% CI = 0.36 to 0.80, Cox P = 0.00206181; OS HR = 0.53, 95% CI = 0.31 to 0.91, Cox P = 0.0219869). (Fig. 2A, B, D). So it is conceivable that high LPAR6 expression is an independent risk factor and leads to a better prognosis in lung cancer patients, and a hazard ratio below 0 indicates LPAR6 expression is a protective factor. Also, high LPAR6 expression significantly impacts DSS in bladder cancer and RFS and DFS in breast cancer (Fig. 2C, E, F). Moreover, three cohorts (GSE19615, GSE9195 and GSE11121) of breast cancer demonstrated that higher expression level of LPAR6 was correlated with a better prognosis potential of DMFS (Fig. 2G-I). And higher LPAR6 expression level was associated with better prognosis potential in some other types of cancer (Fig. 2J-M).

To further analyze the prognostic characteristics of LPAR6 gene in different types of cancer, we employed Kaplan-Meier plotter database to access the LPAR6 prognostic value. Similarly, a better prognosis potential in breast and lung cancer was shown to correlate with higher LPAR6 expression (Fig. 2N-P, T-V).

In addition to microarray analysis data of LPAR6, the RNA-Seq was also used to analyze the prognosis of LPAR6 in various types of cancers via the same database. A better prognosis in breast cancer is shown to be associated with a higher LPAR6 expression level (Fig. 2Q-S). The different correlation patterns between adenocarcinoma and squamous cell carcinoma of lung cancer attracted our attention (Fig. 2V, W). These data confirmed the prognostic value of LPAR6 in some specific types of cancers, that is, the increased or decreased LPAR6 expression has different prognostic values depending on the type of cancers.

In addition to using Kaplan-Meier and PrognoScan plotter databases, TCGA database were also employed to determine the prognostic characteristics of LPAR6 in different types of cancer via GEPIA2. We assessed the relationships between the level of LPAR6 and prognostic potential in 33 types of cancer. LPAR6 expression significantly impacts prognosis in 3 types of cancers, including ACC, LGG (**Supplementary Fig. 1**). High LPAR6 expression levels were associated with a better prognosis of OS in SKCM but have less influence on DFS. These

results demonstrated the prognostic value of LPAR6 in some types of cancers and that differential LPAR6 expression has different prognostic values depending on the type of cancers.

3.3 The expression level of LPAR6 impacts the lung cancer prognosis in different stages and treatments

In this part, we studied the association with the expression level of LPAR6 and different clinical characteristics in order to better disclosure the relevance and mechanisms of the expression level of LPAR6 in cancers, especially in different clinical stages, of lung cancer patients.

We found that high expression of LPAR6 was associated with better OS only in Stage 1 and Stage 2 of LUAD (OS HR = 0.27, *P* = 4.6E-10; OS HR = 0.51, *P* = 0.0073) not in LUSC (Table 1). This interesting phenomenon combines with the different survival rate patterns of LUAD and LUSC in Figs. 2V and 2W may indicate the correlation of LPAR6 expression and the prognosis of different cancers depends on the different mechanisms in the tumorigenesis and development.

Table 1
Correlation of the mRNA expression level of *LPAR6* in different stage and clinical prognostic potential in lung Cancer with different clinicopathological factors.

Clinicopathological Characteristics	Overall survival (n = 364)					
	LUAD (n = 720)			LUSC (n = 524)		
	N	Hazard ratio	P-value	N	Hazard ratio	P-value
Sex						
Female	318	0.39 (0.26–0.58)	**1.4E-10**	129	1.69 (0.94–3.01)	0.075
Male	344	0.66 (0.48–0.93)	**0.015**	342	0.79 (0.59–1.04)	0.087
Smoking history						
Never	143	0.4 (0.17–0.96)	**0.034**	9	—	—
Smoker	246	0.49 (0.3–0.79)	**0.0029**	820	0.89 (0.72–1.09)	0.26
Stage						
1	370	0.27 (0.17–0.42)	**4.6E-10**	172	0.75 (0.49–1.14)	0.17
2	136	0.51 (0.31–0.84)	**0.0073**	100	1.42 (0.76–2.65)	0.27
3	24	2.1 (0.71–6.21)	0.17	43	0.48 (0.24–0.96)	**0.035**
4	4	—	—	0	—	—
Bold values indicate P< 0.05.						

3.4 Low Promoter Methylation Levels of LPAR6 Impacts the Clinicopathological Parameters of Liver Cancer and Lung Cancer in Patients

The lower promoter methylation levels of LPAR6 were detected in the earlier stage, implying that lower promoter methylation levels of LPAR6 were correlated with the earlier stages of the progress of lung cancer (Fig. 3). We also found that late-stage (stage 4) with the lowest promoter methylation levels of LPAR6 in LUSC whereas it is the highest methylation level in entire cancer progress in LUAD cohorts (stage 1–4) (Fig. 3A, 3E), and the lowest promoter methylation levels of LPAR6 appears in an earlier stage (stage 2) of LUAD while in the late stage of LUSC. What interested us is that the same pattern was detected in nodal metastasis analysis, which implies that in the later stage, the promoter methylation levels of LPAR6 are correlated with nodal metastasis in some way (Fig. 3D, 3H). The promoter methylation levels of LPAR6 share a similar pattern in LUAD and LUSC among

different races and different ages respectively, that is, both in the African-America group and younger group of these two cohorts with the lowest promoter methylation levels of LPAR6 (Fig. 3B, 3F).

3.5 Interaction network of LPAR6

An interaction network of LPAR6 was constructed to determine potential interactions between LPAR6 and other cancer-associated proteins. The data demonstrated that LPAR6 has co-expression with 19 proteins, shared protein domains with ADRB2 and physical interactions with DMD (dystrophin) (Fig. 4A). LinkedOmics were then used to analysis the genes that co-expressed with LPAR6 in lung cancers. The volcano plot elucidated that the expression of genes were negative correlated with that of LPAR6 [green spot; FDR < 0.05], while genes expression is positively correlated with LPAR6 (red spot; FDR < 0.05; Fig. 4B). The top 50 positively and negatively correlated genes are showed in Fig. 4B. These results imply that LPAR6 serves an important role in cancer development. Biological process and molecular function analyses were conducted using gene set enrichment analysis, which showed that LPAR6-associated DEGs were involved in several kinds of immune biology process such as ‘interleukin production’, ‘respiratory burst’, ‘leukocyte proliferation’, ‘T cell activation’, ‘adaptive immune response’ were involved in LUAD and LUSC respectively. (Fig. 5). All these data indicate that LPAR6 serves a key role in immune system activation, cellular responses to stimulation, metabolism and many other processes.

3.6 The expression level of LPAR6 is correlated with immune infiltration level in lung cancers

TILs have been proved as an independent predictor of survival in cancers [46, 47]. So, in this study, we determined whether the mRNA expression level of LPAR6 correlates with the immune infiltration levels in various types of cancer. We analyzed the correlations of LPAR6 expression with immune infiltration levels in nearly forty types of cancer. The results show that the expression level of LPAR6 has significant negative correlations with tumor purity in 26 types of cancer which indicating LPAR6 somehow related to recruiting lymphocytes to tumor and significant correlations with B cell infiltration levels in 13 types of cancers. In addition, the expression level of LPAR6 has significant correlations with infiltrating levels of CD8 + T cells in 24 types of cancer, CD4 + T cells in 26 types of cancer, macrophages in 20 types of cancer, neutrophils in 33 types of cancer, and dendritic cells in 21 types of cancer. **(Supplementary Table 3 and Supplementary Fig. 2).**

Given the correlation of the expression level of LPAR6 with immune infiltration level in diverse types of cancer, we next investigated the distinct types of cancers in which LPAR6 was correlated with prognosis and immune infiltration. Tumor purity is a crucial factor that influences the analysis of immune infiltration in clinical tumor samples by genomic approaches [34, 41]. So we selected the cancer types in which LPAR6 expression levels have a significant negative correlation with tumor purity in TIMER and a significant correlation with prognosis. Interestingly, we found that the expression level of LPAR6 expression correlates with better OS and high immune infiltration levels in breast cancer, liver cancer and LUAD but not in LUSC.

The LPAR6 expression level of LUAD and LUSC are all significantly negatively related to tumor purity (Fig. 6). LPAR6 expression level has significant positive correlations with the infiltrating levels of B cell, CD8 + T cell, CD4 + T cells, Macrophages, Neutrophils and DCs in LUAD (Fig. 6). What interested us is that the correlation with immune cells demonstrated a different pattern in LUAD and LUSC of lung cancers. These findings strongly

suggest that LPAR6 plays a specific role in immune infiltration in different types of lung cancer, and leads to a better prognosis in LUAD instead of in LUSC.

3.7 Correlation Analysis Between LPAR6 Expression and Immune Marker Sets

To study the association between LPAR6 and different types of TIICs, we focused on the correlations between the expression level of LPAR6 and immune marker sets of various immune cells of LUAD and LUSC. The correlations between LPAR6 expression level and immune marker gene sets of different immune cells, including CD8 + T cells, T cells (general), B cells, monocytes, TAMs, M1 and M2 macrophages, neutrophils, NK cells and DCs were determined in LUAD and LUSC (**Table 3 and** Fig. 7). We also investigated the different types of T cells (Th1, Th2, Tfh, Th17, Tregs and exhausted T cells). After adjustment by purity, the correlation results revealed the LPAR6 expression level was significantly correlated with most immune marker sets of various immune cells and different subtypes of T cells, especially effect T cells in LUAD. However, none of these gene markers was significantly correlated with the LPAR6 expression level in LUSC and other cancer with poor prognosis (**Table 3 and** Fig. 7).

These results demonstrated that the mRNA expression levels of the marker genes in T cells (general, CD8+, Naive T, Effector T), natural killer cell, M1 macrophages and DCs have strong correlations with LPAR6 expression in LUAD (**Table 3**). More specifically, we demonstrated NOS2, IRF5, PTGS2 of M1 phenotype are significantly correlate with LPAR6 expression in LUAD ($P < 0.0001$; Fig. 4A–H). It is reported that M1 could prevent tumor development. In-depth studies need to be done on whether LPAR6 is a crucial factor that mediating the de-polarization of macrophages and remodel tumor microenvironment. In addition, for Treg cells, LPAR6 does not demonstrate a correlation with the Tregs markers such as STAT5B in LIHC (**Table 3**). Furthermore, we determined the association between the expression level of LPAR6 and the above marker sets of monocytes and various types of T cells in normal and tumor tissue in LUAD and LUSC. (**Supplementary-Table 4**, Fig. 8).

3.8 Different correlation patterns between tumor and normal tissue in LUAD patients

The more interesting thing is that the expression levels of most marker sets of these immunocytes have strong correlations with LPAR6 expression in tumor tissue of LUAD patients. In the LUSC, there was no significant correlation between LPAR6 and markers of immune cells **(**Fig. 9, **Supplementary-Table 4**). This finding suggests that there are different correlation patterns between tumor and normal tissue in LUAD patients. This exciting finding indicates that LPAR6 may regulate macrophage de-polarization in the tumor microenvironment of the LUAD and LPAR6 might be a novel target for LUAD therapy. High LPAR6 expression relates to a high infiltration level of DCs in the tumor tissue of LUAD patients, DC markers such as HLA-DQB1, CD1C and NRP1 show significant correlations with LPAR6 expression both in the tumor tissue in LUAD (**Supplementary-Table 4**). These results further reveal that there is a strong relationship between LPAR6 and DCs infiltration.

3.9 Higher expression of LPAR6 was correlated with clinicopathological parameters in LUAD cohort and was

correlated with increased overall survival (OS) of LUAD and LUSC patients

We analyzed the protein level of LPAR6 in two independent lung cancer patient cohorts with 74 and 77 paired lung cancer and normal tissues respectively. LPAR6 is mainly expressed in the cytoplasm of the cells (Fig. 10A), and the protein level was lower in the lung cancer tissues compared with the normal tissues (Fig. 10B, D). Next step, we investigated the relationship between the LPAR6 protein level and the clinical characteristics of the LUAD and LUSC patient cohorts. Lung cancer patients with higher LPAR6 levels demonstrated better OS than those patients with relatively lower levels in LUAD patient cohorts, but not in LUSC patient cohorts (Fig. 10C, E). Moreover, we found that lower LPAR6 was negatively correlated with the clinical stage of lung cancer and the lymph node metastasis of patients (Fig. 10F, G).

In summary, we demonstrated that the LPAR6 was downregulated in the tumor tissue of LUAD patients and its expression was positive associated with the overall survival for LUAD patients base on the databases and TMA cohorts. The results further confirm that LPAR6 is specifically correlated with immune infiltrating cells in LUAD which suggests that LPAR6 plays a vital role in immune cells recruiting in the tumor tissue in LUAD patients. LPAR6 and its modulation on tumor microenvironment may serve as a novel therapeutic target for LUAD.

4. Discussion

LPA receptors are GPCR that bind to the LPA and trigger multiple downstreaming cellular responses, including cell proliferation, cytoskeletal rearrangements, apoptosis and motility [48–50]. Previously, five LPA receptors (*LPAR*1-5) are well characterized and extensively studied [51]. LPAR6 is a recently determined GPCR, alias as ARWH1, HYPT8, LAH3, P2RY5, at first was considered as purinergic receptor P2Y5 that involved in inherited hair loss [23, 52]. Although LPAR6 has not been extensively studied, it was reported that the LPAR6 suppresses tumor cell migration in colorectal cancer [28], and the expression of LPAR6 was decreased in P53-mutated cases [29]. It was also reported that the LPA axis plays an important role in HCC by recruiting and trans-differentiating of peritumoral fibroblasts into TAMs [53, 54]. This offers scientists a promising hint that LPAR6 is involved in the TME. Immunotherapy is a new genre of treatment for patients and has a tightly association with TME [29].

In this study, we announced that different expression levels of LPAR6 are associated with the prognostic potential in various cancer types. Higher level of LPAR6 is associated with a better prognosis in three types of cancers, including liver cancer, lung cancer and breast cancer. Moreover, our data demonstrated that the immune infiltration levels and diverse immune marker sets of the different subtypes of lung cancers (LUAD and LUSC) are associated with the expression level of LPAR6. To this end, our study provides insights into elucidating the potential role of LPAR6 in tumor immunology and its usage as a biomarker and novel therapy target for LUAD.

In this work, we determined the LPAR6 expression levels and constructed a systematic prognostic landscape in various types of cancers by using independent datasets in Oncomine and 33 type cancers of TCGA data in GEPIA2. The variation expression level of LPAR6 between cancer and normal tissues was observed in many cancer types. Based on the Oncomine database, we found that LPAR6, compared to normal tissues, was highly

expressed in brain and CNS, kidney, gastric cancer, leukemia, lymphoma, liver and pancreatic cancer while some data sets showed that LPAR6 has a lower mRNA expression level in bladder, breast, cervical, colorectal, esophageal, lung and prostate cancer (Fig. 1A). However, the redetermination of the TCGA data demonstrated that LPAR6 expression was higher expressed in ESCA, KIRC, KIRP and THCA, but significantly lower expressed in BLCA, COAD, BRCA, HNSC, KICH, PRAD, LUAD, UCEC, READ and slightly lower in LIHC compared with adjacent normal tissues (Fig. 1B). The vary in the expression levels of *LPAR6* in different types of cancer among various databases might be a reflection in data collection approaches and underlying mechanisms involved in different biological properties. Nevertheless, in these databases, we found similar prognostic associations between LPAR6 expression in bladder, breast, cervical, colorectal, esophageal, lung and prostate cancers. Investigation of the TCGA database enclosed that the higher LPAR6 expression level is correlated with better prognostic potential in ACC, LGG, SKCM (**Supplementary-Figure2**). Furthermore, the determination of patient cohorts from PrognoScan and Kaplan-Meier Plotter demonstrated a high level of *LPAR6* expression is correlated with better prognosis in breast, lung, bladder, colorectal, eye and ovarian cancer (Fig. 2). In two datasets of PrognoScan, high LPAR6 expression levels could be considered as an independent risk factor for better prognosis in LUAD. Moreover, a high level of LPAR6 expression was shown to be correlated with a better prognosis of LUAD in the early stage with the lowest HR [0.27 (0.17–0.42)] for a better OS when LPAR6 was highly expressed in LUAD, rather than in LUSC. These together strongly suggest that LPAR6 could be a prognostic biomarker in LUAD.

Another crucial aspect of this work is that the mRNA expression level of LPAR6 is correlated with diverse immune infiltration levels in cancer, especially in LUAD. Here, we demonstrate that there's a strong positive correlation between the infiltration level of T cells (CD8 + and CD4+), neutrophils, macrophages and DCs and LPAR6 expression in LUAD (Figs. 3A, 3C). Moreover, the correlation patterns of the infiltration level are different in two kinds of lung cancers (LUAD and LUSC). The correlation between LPAR6 expression and the marker genes of immune cells implicates the role of LPAR6 in regulating tumor immunology in these types of cancers. A possible explanation for this striking effect might be that LPAR6 orchestrates the function of multiple immune marker gene sets. This supports the argument that the LPAR6 expression levels are important contributors to human malignancies and indicating the prognosis of specific types of cancer.

Firstly, gene markers of M1 macrophages such as PTGS2 and IRF5 show significant correlations with LPAR6 expression in LUAD respectively (Tables 2). Since macrophages are functionally plastic cells. Type 1 macrophages (M1) producing type 1 cytokines prevent tumors from developing, whereas type 2 macrophages (M2) inducing type 2 cytokines facilitate tumor growth. Especially in the tumor tissue of LUAD, both NOS2 and IRF5 show significant correlations with LPAR6 expression and PTGS2 shows a significant correlation with LPAR6 expression in the tumor tissue (**Supplementary-Table 4**). These results reveal the potential regulating role of LPAR6 in de-polarization macrophages against tumor that activated macrophages can be re-polarized into opposite functional phenotypes by microenvironmental modifications and then inhibit tumor growth.

Table 2
Correlation analysis between *LPAR6* and relate markers of immune cells

Description	Gene markers	LUAD				LUSC			
		None		Purity		None		Purity	
		Cor	P	Cor	P	Cor	P	Cor	P
CD8 + T cell	CD8A	0.363	***	0.238	***	0.121	*	0.065	0.157
	CD8B	0.366	***	0.281	***	0.231	***	0.196	***
T cell (general)	CD3D	0.451	***	0.318	***	0.197	***	0.136	*
	CD3E	0.434	***	0.283	***	0.163	**	0.092	0.045
	CD2	0.49	***	0.358	***	0.171	**	0.101	0.0277
Naive T-Cell	CCR7	0.39	***	0.222	***	0.175	***	0.109	0.0175
	LEF1	0.351	***	0.241	***	-0.002	0.962	0.014	0.766
	TCF7	0.237	***	0.102	0.0232	0.095	0.0336	0.049	0.289
	SELL	0.421	***	0.26	***	0.187	***	0.115	0.12
Effector T-Cell	CX3CR1	0.41	***	0.353	***	0.113	0.0113	0.055	0.23
	FGFBP2	0.247	***	0.185	***	-0.04	0.378	-0.02	0.656
	FCGR3A	0.448	***	0.354	***	0.042	0.35	-0.044	0.34
Effector memory T-Cell	PDCD1	0.316	***	0.175	***	0.112	0.0121	0.045	0.323
	DUSP4	-0.074	0.0915	-0.075	0.0966	-0.017	0.707	-0.057	0.212
	GZMK	0.444	***	0.309	***	0.172	**	0.106	0.0204
	GZMA	0.408	***	0.295	***	0.197	***	0.143	*
	IFNG	0.304	***	0.201	***	0.101	0.0235	0.061	0.183
Resident memory T-Cell	CD69	0.518	***	0.423	***	0.247	***	0.192	***
	ITGAE	0.295	***	0.228	***	0.109	0.0149	0.09	0.0493
	CXCR6	0.434	***	0.305	***	0.161	**	0.095	0.0389
	MYADM	0.162	**	0.064	0.156	-0.132	*	-0.197	***
B cell	CD19	0.341	***	0.192	***	0.157	**	0.083	0.0694
	CD79A	0.312	***	0.171	**	0.155	**	0.076	0.096

TAM, tumor-associated macrophage; Th, T helper cell; Tfh, Follicular helper T cell; Treg, regulatory T cell; Cor, R value of Spearman's correlation; None, correlation without adjustment. Purity, correlation adjusted by purity.

P< 0.01;P< 0.001;***P< 0.0001.*

Description	Gene markers	LUAD				LUSC			
		None		Purity		None		Purity	
		Cor	P	Cor	P	Cor	P	Cor	P
Monocyte	CD86	0.55	***	0.455	***	0.164	**	0.079	0.085
	CD115 (CSF1R)	0.495	***	0.388	***	0.071	0.111	-0. 031	0.498
TAM	CCL2	0.424	***	0.331	***	0.148	**	0.086	0.0611
	CD68	0.387	***	0.291	***	0.012	0.785	-0.087	0.0576
	IL10	0.523	***	0.433	***	0.211	***	0.151	**
M1 Macrophage	INOS (NOS2)	0.14	*	0.075	0.0955	0.104	0.0203	0.106	0.0203
	IRF5	0346	***	0.254	***	-0. 101	0.0236	-0.129	**
	COX2 (PTGS2)	0.009	0.833	0.017	0.705	0.27	***	0.244	***
M2 Macrophage	CD163	0.376	***	0.281	***	0.032	0.472	-0.058	0.209
	VSIG4	0.438	***	0.358	***	0.061	0.171	-0.021	0.649
	MS4A4A	0.501	***	0.412	***	0.109	0.0145	0.028	0.536
Neutrophils	CD66b (CEACAM8)	0.114	*	0.09	0.0464	0.023	0.613	0.006	0.894
	CD11b (ITGAM)	0.405	***	0.29	***	0.091	0.0412	-0.006	0.898
	CCR7	0.39	***	0.222	***	0.175	***	0.109	0.0175
Natural killer cell	KIR2DL1	0.117	*	0.064	0.155	0.081	0.0704	0.052	0.258
	KIR2DL3	0.209	***	0.13	*	0.013	0.776	0.013	0.776
	KIR2DL4	0.179	***	0.11	0.0145	0.08	0.0744	0.039	0.4
	KIR3DL1	0.149	**	0.075	0.098	0.005	0.902	-0.048	0.294
	KIR3DL2	0.168	**	0.078	0.083	0.015	0.737	-0.038	0.41
	KIR3DL3	0.039	0.38	0.006	0.899	-0.116	*	-0.142	*
	KIR2DS4	0.143	*	0.065	0.149	0.052	0.245	0.026	0.572

TAM, tumor-associated macrophage; Th, T helper cell; Tfh, Follicular helper T cell; Treg, regulatory T cell; Cor, R value of Spearman's correlation; None, correlation without adjustment. Purity, correlation adjusted by purity.

P< 0.01;P< 0.001;***P< 0.0001.*

Description	Gene markers	LUAD				LUSC			
		None		Purity		None		Purity	
		Cor	P	Cor	P	Cor	P	Cor	P
Dendritic cell	HLA-DPB1	0.463	***	0.353	***	0.098	0.0279	0.014	0.759
	HLA-DQB1	0.315	***	0.195	***	0.098	0.0279	0.014	0.759
	HLA-DRA	0.476	***	0.376	***	0.135	*	0.062	0.178
	HLA-DPA1	0.447	***	0.343	***	0.106	0.0172	0.029	0.521
	BDCA-1 (CD1C)	0.382	***	0.294	***	0.196	***	0.131	*
	BDCA-4 (NRP1)	0.18	***	0.137	*	0.052	0.247	-0.014	0.767
	CD11c (ITGAX)	0.474	***	0.364	***	0.168	**	0.082	0.074
Th1	TBX21 (T-bet)	0.355	***	0.216	***	0.119	*	0.051	0.266
	STAT4	0.394	***	0.267	***	0.195	***	0.122	*
	STAT1	0.193	***	0.075	0.094	0.032	0.477	-0.018	0.689
	IFNG (IFN-g)	0.304	***	0.201	***	0.101	0.0235	0.061	0.183
	TNF-a (TNF)	0.414	***	0.291	***	0.277	***	0.229	***
Th2	GATA3	0.365	***	0.231	***	0.187	***	0.143	*
	STAT6	0.007	0.873	0.019	0.681	0.257	***	0.259	***
	STAT5A	0.459	***	0.33	***	0.15	**	0.082	0.0722
	IL13	0.209	***	0.128	0.0213	0.076	0.0818	0.037	0.423
Tfh	BCL6	0.022	0.612	0.018	0.684	0.08	0.0729	0.105	0.0223
	IL21	0.118	**	0.038	0.402	0.034	0.452	-0.013	0.782
Th17	STAT3	-0.138	**	-0.147	**	0.129	*	0.109	0.0168
	IL17A	0.177	***	0.11	0.014	0.051	0.254	0.025	0.58
Treg	FOXP3	0.364	***	0.207	***	0.145	*	0.063	0.172

TAM, tumor-associated macrophage; Th, T helper cell; Tfh, Follicular helper T cell; Treg, regulatory T cell; Cor, R value of Spearman's correlation; None, correlation without adjustment. Purity, correlation adjusted by purity.

P< 0.01;P< 0.001;***P< 0.0001.*

Description	Gene markers	LUAD				LUSC			
		None		Purity		None		Purity	
		Cor	P	Cor	P	Cor	P	Cor	P
	CCR8	0.382	***	0.242	***	0.162	**	0.083	0.0706
	STAT5B	0.212	***	0.18	***	-0.071	0.114	-0.076	0.096
	TGFB1 (TGFb)	0.304	***	0.201	***	0.123	**	0.123	***
T cell exhaustion	PDCD1 (PD-1)	0.316	***	0.175	***	0.112	0.0121	0.045	0.323
	CTLA4	0.444	***	0.304	***	0.217	***	0.152	**
	LAG3	0.275	***	0.152	***	0.095	0.0329	0.034	0.457
	HAVCR2 (TIM-3)	0.539	***	0.442	***	0.094	0.0357	0.008	0.867
	GZMB	0.268	***	0.15	***	0.137	**	0.077	0.0926

TAM, tumor-associated macrophage; Th, T helper cell; Tfh, Follicular helper T cell; Treg, regulatory T cell; Cor, R value of Spearman's correlation; None, correlation without adjustment. Purity, correlation adjusted by purity.

P< 0.01;P< 0.001;***P< 0.0001.*

Secondly, our results indicated that LPAR6 has the potential to activate CD8 + T cell, naive T-cell, effector T-cell and natural killer cell and inactivate Tregs, and decrease T cell exhaustion. CD8A, a crucial surface protein on T cells, is highly correlated with LPAR6 expression in LUAD which are types of cancers with better prognosis. And CD8A did not demonstrate a significant correlation pattern in LUSC (Table 3). This pattern also occurs with the general T cell markers such as CD3D, CD3E, CD2 and most markers of naive T-cell, effector T-cell, effector memory T-cell and natural killer cells. Such as LEF1 which has been proved to be a predictor of better treatment response in AML, because high LEF1 expression level was associated with favorable relapse-free survival in patients and predicted a significantly better overall survival for AML patients [55].

Thirdly, different correlation patterns can be found between LPAR6 expression and the regulation of several markers of T helper cells (Th1, Th2, Tfh, and Th17) in these different cancers. IFN-g is a Th1 cytokine with both pro-and anti-cancer properties [56] which are highly correlated with LPAR6 expression in LUAD, whereas did not demonstrate significant correlations in LUSC (Table 3). IL-13 is an important immunoregulatory cytokine mainly produced by activated type II helper T cells and is widely involved in tumorigenesis and development, fibrosis and inflammation [57, 58]. We found that IL-13 is highly correlated with *LPAR6* expression in LUAD, but did not demonstrate significant correlations in LUSC (adjusted by purity), and a similar situation is in the IL-21. So these would be explanations that why LPAR6 indication poor prognosis in LUSC and a better prognosis in LUAD.

All these correlations above could be indications of a potential mechanism where LPAR6 regulates T cell functions in LUAD. Together these findings suggest that the LPAR6 plays an important role in the recruitment and regulation of effective T cells infiltrating in LUAD leading to a better prognosis.

5. Conclusions

In this study, we offered a potential explanation for the mechanism that why LPAR6 expression correlates with immune infiltration level and better prognostic potential in some specific types of cancer, especially in LUSC. Hence, the interactions between LPAR6 and the immunocytes in the tumor microenvironment could be a potential mechanism for the correlation of LPAR6 expression with immune infiltration level and better prognosis in LUAD patients.

Abbreviations

TMA	Tissue microarrays
TCGA	The Cancer Genome Atlas
DEG	Differentially expressed gene
TIICs	Tumor-infiltrating immune cells
TILs	Tumor-infiltrating lymphocytes
TINs	Tumor-infiltrating neutrophils
TAMs	Tumor association macrophages
FDR	False Discovery Rate
TME	Tumor microenvironment

Declarations

Ethics approval and consent to participate

This project was permitted by Independent Ethics Committee of Shanghai Jiao Tong University School of Medicine.

Consent for publication

Not applicable

Availability of data and materials

All data generated or analyzed during this study are included in this published article and its supplementary information files.

Conflict of interest

The authors declare there is none conflicts of interest. This research conforms to all the laws and ethical guidelines that apply in the country where I carried it out.

Authors' contributions

J. H. contributed to idea, conception, and study design. J. H. collected and analyzed the datasets, performed TMA analysis. J. H., M.M. and R.G. wrote the manuscript and generating the figures. H. W. revised and proofread the article.

Funding

This project is funded by the grants of National Natural Science Foundation of China (NSFC 81702730) and Start-up Plan for New Young Teacher of SHSMU (KJ30214190026) of JH and National Natural Science Foundation of China (NSFC 81630086), National Key Research & Development Program of China (2018YFC2000700) of HW.

Acknowledgments

We would like to thank to the funder.

Database	Website	Reference
Oncomine	https://www.oncomine.org/resource/login.html	32
GEPIA2	http://gepia.cancer-pku.cn/	34
PrognoScan	http://dna00.bio.kyutech.ac.jp/PrognoScan/	33
Kaplan-Meier plotter	http://kmplot. com/analysis/	35
UALCAN	http://ualcan.path.uab.edu	36
GeneMANIA	http://genemania.org/	37
LinkedOmics database	http://www.linkedomics.org/login.php	38
TIMER	https://cistrome.shinyapps.io/timer/	40

References

1. Siegel RL, Miller KD, Jemal A. Cancer statistics, 2018. CA Cancer J Clin 2018.
2. American Cancer Society. Key statistics for lung cancer. www.cancer.org/cancer/non-small-cell-lung-cancer/about/key-statistics.html.
3. Yang L, Wang L, Zhang Y. Immunotherapy for lung cancer: advances and prospects. Am J Clin Exp Immunol. 2016; 5: 1-20.

4. Dela Cruz CS, Tanoue LT, Matthay RA. Lung cancer: epidemiology, etiology, and prevention. Clin Chest Med. 2011; 32 (4): 605-44.
5. Gelsomino F, Lamberti G, Parisi C, Casolari L, Melotti B, Sperandi F, Ardizzoni A. The evolving landscape of immunotherapy in small-cell lung cancer: A focus on predictive biomarkers. Cancer Treat Rev. 2019; 79: 101887.
6. Vafadar S. Immunotherapy for non-small cell lung cancer. JAAPA. 2019; 32 (9): 37-42.
7. Neeve SC, Robinson BW, Fear VS. The role and therapeutic implications of T cells in cancer of the lung. Clin Transl Immunology. 2019; 8(8): e1076.
8. Steven A, Fisher SA, Robinson BW. Immunotherapy for lung cancer. Respirology 2016; 21: 821-33.
9. Charles Schmidt. Immunology: Another shot at cancer. Nature. 2015; 527 (7578): S105-7.
10. Barbee MS, Ogunniyi A, Horvat TZ, Dang TO. Current status and future directions of the immune checkpoint inhibitors ipilimumab, pembrolizumab, and nivolumab in oncology. Ann Pharmacother. 2015; 49 (8): 907-37.
11. Garon EB, Rizvi NA, Hui R, Leighl N, Balmanoukian AS, Eder JP, et al. Pembrolizumab for the treatment of non-small-cell lung cancer. N Engl J Med. 2015; 372 (21): 2018–28.
12. Ravelli A, Roviello G, Cretella D, Cavazzoni A, Biondi A, Cappelletti MR, et al. Tumor-infiltrating lymphocytes and breast cancer: Beyond the prognostic and predictive utility. Tumour Biol. 2017; 39 (4): 1010428317695023.
13. Stanton SE, Disis ML. Clinical significance of tumor-infiltrating lymphocytes in breast cancer. J Immunother Cancer. 2016; 4: 59.
14. Choi J, Gyamfi J, Jang H, Koo JS. The role of tumor associated macrophage in breast cancer biology. Histol Histopathol. 2018; 33(2): 133-45.
15. Tariq M, Zhang J, Liang G, Ding L, He Q, Yang B. Macrophage Polarization: Anti-Cancer Strategies to Target Tumor-Associated Macrophage in Breast Cancer. J Cell Biochem. 2017; 118 (9): 2484-501.
16. Santoni M, Romagnoli E, Saladino T, Foghini L, Guarino S, Capponi M, et al. Triple negative breast cancer: Key role of Tumor-Associated Macrophages in regulating the activity of anti-PD-1/PD-L1 agents. Biochim Biophys Acta Rev Cancer. 2018; 1869 (1): 78-84.
17. Benevides L, da Fonseca DM, Donate PB, Tiezzi DG, De Carvalho DD, de Andrade JM, et al. IL17 Promotes Mammary Tumor Progression by Changing the Behavior of Tumor Cells and Eliciting Tumorigenic Neutrophils Recruitment. Cancer Res. 2015; 75 (18): 3788-99.
18. Toor SM, Syed Khaja AS, El Salhat H, Faour I, Kanbar J, Quadri AA, et al. Myeloid cells in circulation and tumor microenvironment of breast cancer patients. Cancer Immunol Immunother. 2017; 66 (6): 753-64.
19. Ban Y, Mai J, Li X, Mitchell-Flack M, Zhang T, Zhang L et al. Targeting Autocrine CCL5-CCR5 Axis Reprograms Immunosuppressive Myeloid Cells and Reinvigorates Antitumor Immunity. Cancer Res. 2017; 77 (11): 2857-68.
20. Waniczek D, Lorenc Z, Snietura M, Wesecki M, Kopec A, Muc-Wierzgon M. Tumor associated macrophages and regulatory T cells infiltration and the clinical outcome in colorectal cancer. Arch Immunol Ther Exp. 2017; 65: 445–54.

21. Lopane C, Agosti P, Gigante I, et al. Implications of the lysophosphatidic acid signaling axis in liver cancer. Biochim Biophys Acta Rev Cancer. 2017; 1868 (1): 277-82.
22. Bailey KA, Klymenko Y, Feist PE, Hummon AB, Stack MS, Schultz ZD. Chemical analysis of morphological changes in lysophosphatidic acid-treated ovarian cancer cells. Sci Rep. 2017; 7 (1): 15295.
23. Shimomura Y, Wajid M, Ishii Y, Shapiro L, Petukhova L, Gordon D, et al. Disruption of P2RY5, an orphan G protein-coupled receptor, underlies autosomal recessive woolly hair. Nat Genet. 2008; 40 (3): 335-9.
24. Taniguchi R, Inoue A, Sayama M, Uwamizu A, Yamashita K, Hirata K, Yoshida M, et al. Structural insights into ligand recognition by the lysophosphatidic acid receptor LPA6. Nature. 2017; 548 (7667): 356-60.
25. Ketscher A, Jilg CA, Willmann D, et al. LSD1 controls metastasis of androgen-independent prostate cancer cells through PXN and LPAR6. Oncogenesis. 2014; 3: e120.
26. Mazzocca A, Dituri F, De Santis F, Filannino A, Lopane C, Betz RC, et al. Lysophosphatidic acid receptor LPAR6 supports the tumorigenicity of hepatocellular carcinoma. Cancer Res. 2015; 75 (3): 532-43.
27. Sokolov E, Eheim AL, Ahrens WA, et al. Lysophosphatidic acid receptor expression and function in human hepatocellular carcinoma. J Surg Res. 2013; 180 (1): 104-13.
28. Takahashi K, Fukushima K, Onishi Y, Inui K, Node Y, Fukushima N, et al. Lysophosphatidic acid (LPA) signaling via LPA4 and LPA6 negatively regulates cell motile activities of colon cancer cells. Biochem Biophys Res Comm. 2017; 483 (1): 652-7.
29. Katkoori VR, Shanmugam C, Jia X, Vitta SP, Sthanam M, Callens T, et al. Prognostic significance and gene expression profiles of p53 mutations in microsatellite- stable stage III colorectal adenocarcinomas. PloS One. 2012; 7(1): e30020.
30. Ishii S, Hirane M, Fukushima K, et al. Diverse effects of LPA4, LPA5 and LPA6 on the activation of tumor progression in pancreatic cancer cells. Biochem Biophys Res Comm. 2015; 461(1): 59-64.
31. Hanauer DA, Rhodes DR, Sinha-Kumar C, Chinnaiyan AM. Bioinformatics approaches in the study of cancer. Curr Mol Med. 2007; 7 (1): 133-41.
32. Rhodes DR, Kalyana-Sundaram S, Mahavisno V, Varambally R, Yu J, Briggs BB, et al. Oncomine 3.0: genes, pathways, and networks in a collection of 18,000 cancer gene expression profiles. Neoplasia. 2007; 9 (2):166-80.
33. Tang, Z, Kang B, Li C, Chen T, Zhang Z. GEPIA2: an enhanced web server for large-scale expression profiling and interactive analysis. Nucleic Acids Res. 2019; 47(W1): W556-60.
34. Hideaki Mizuno, Kunio Kitada, Kenta Nakai and Akinori Sarai. PrognoScan: a new database for meta-analysis of the prognostic value of genes. BMC Medical Genomics. 2009; 2:18.
35. Lanczky A, Nagy A, Bottai G, Munkacsy G, Szabo A, Santarpia L, et al. miRpower: a web-tool to validate survival-associated miRNAs utilizing expression data from 2178 breast cancer patients. Breast Cancer Res Treat. 2016; 160 (3): 439–46.
36. Chandrashekar DS, Bashel B, Balasubramanya SAH, Creighton CJ, Rodriguez IP, Chakravarthi BVSK and Varambally S. UALCAN: A portal for facilitating tumor subgroup gene expression and survival analyses. Neoplasia. 2017; 19 (8): 649-58.
37. Warde-Farley D, Donaldson SL, Comes O, Zuberi K, Badrawi R, Chao P, Franz M, Grouios C, Kazi F, Lopes CT, et al. The GeneMANIA prediction server: Biological network integration for gene prioritization and predicting

gene function. Nucleic Acids Res. 2010; 38: W214-20.

38. Vasaikar SV, Straub P, Wang J and Zhang B. LinkedOmics: Analyzing multi-omics data within and across 32 cancer types. Nucleic Acids Res. 2018; 46: D956-63.
39. Wang J, Vasaikar S, Shi Z, Zhang B and Greer M. WebGestalt: A more comprehensive, powerful, flexible and interactive gene set enrichment analysis toolkit. Nucleic Acids Res. 2017; 45:W130-37.
40. Sousa S, Maatta J. The role of tumour-associated macrophages in bone metastasis. J Bone Oncol. 2016; 5:135-8.
41. Aran D, Sirota M, Butte AJ. Systematic pan-cancer analysis of tumour purity. Nat Commun. 2015; 6:8971.
42. Li T, Fan J, Wang B, Traugh N, Chen Q, Liu JS, et al. TIMER: a web server for comprehensive analysis of tumor-infiltrating immune cells. Cancer Res. 2017; 77: e108-10.
43. Li B, Severson E, Pignon JC, Zhao H, Li T, Novak J, et al. Comprehensive analyses of tumor immunity: implications for cancer immunotherapy. Genome Biol. 2016; 17(1): 174.
44. Danaher P, Warren S, Dennis L, D'Amico L, White A, Disis ML, et al. Gene expression markers of Tumor Infiltrating Leukocytes. J Immunother Cancer. 2017; 5:18.
45. Chen P, Duan X, Li X, Li J, Ba Q, Wang H. HIPK2 suppresses tumor growth and progression of hepatocellular carcinoma through promoting the degradation of HIF-1α. Oncogene. 2020 Apr;39(14):2863-2876.
46. Azimi F, Scolyer RA, Rumcheva P, MoncrieffM, Murali R, McCarthy SW, et al. Tumor-infiltrating lymphocyte grade is an independent predictor of sentinel lymph node status and survival in patients with cutaneous melanoma. J Clin Oncol. 2012; 30: 2678-83.
47. Ohtani H. Focus on TILs: prognostic significance of tumor infiltrating lymphocytes in human colorectal cancer. Cancer Immun. 2007; 7:4.
48. Mills GB and Moolenaar WH. The emerging role of lysophosphatidic acid in cancer. Nat Rev Cancer. 2003; 3: 582-91.
49. van Corven EJ, Groenink A, Jalink K, Eichholtz T, Moolenaar WH. Lysophosphatidate- induced cell proliferation: identification and dissection of signaling pathways mediated by G proteins. Cell. 1989; 59: 45-54.
50. Moolenaar WH, van Meeteren LA, Giepmans BN. The ins and outs of lysophosphatidic acid signaling. Bioessays. 2004; 26: 870-81.
51. Choi JW, Herr DR, Noguchi K, Yung YC, Lee CW, Mutoh T, et al. LPA receptors: subtypes and biological actions. Annu Rev Pharmacol Toxicol. 2010; 50: 157-86.
52. Pasternack SM, von Kugelgen I, Al Aboud K, Lee YA, Ruschendorf F, Voss K, et al. G protein-coupled receptor P2Y5 and its ligand LPA are involved in maintenance of human hair growth. Nat Genet. 2008; 40: 329-34.
53. Mazzocca A, Dituri F, De Santis F, Filannino A, Lopane C, Betz RC, et al. Lysophosphatidic acid receptor LPAR6 supports the tumorigenicity of hepatocellular carcinoma. Cancer Res. 2015; 75 (3): 532-43.
54. Mazzocca A, Dituri F, Lupo L, Quaranta M, Antonaci S,Giannelli G. Tumorsecreted lysophostatidic acid accelerates hepatocellular carcinoma progression by promoting differentiation of peritumoral fibroblasts in myofibroblasts. Hepatology. 2011; 54: 920-30.
55. Fu Y, Zhu H, Wu W, et al. Clinical significance of lymphoid enhancer- binding factor 1 expression in acute myeloid leukemia. Leuk Lymphoma. 2014; 55(2): 371-377.

56. Ganapathi SK, Beggs AD, Hodgson SV, Kumar D. Expression and DNA methylation of TNF, IFNG and FOXP3 in colorectal cancer and their prognostic significance. Br J Cancer. 2014; 111 (8): 1581-9.

57. Fichtner-Feigl S, Strober W, Kawakami K, Puri RK, Kitani A. IL-13 signaling through the IL-13 alpha2 receptor is involved in induction of TGF-beta1 production and fibrosis. Nature medicine. 2006; 1 (1): 99-106.

58. Shimamura T, Fujisawa T, Husain SR, Joshi B, Puri RK. Interleukin 13 mediates signal transduction through interleukin 13 receptor alpha2 in pancreatic ductal adenocarcinoma: role of IL-13 Pseudomonas exotoxin in pancreatic cancer therapy. Clinical cancer research. 2010; 2 (2): 577-86.

Figures

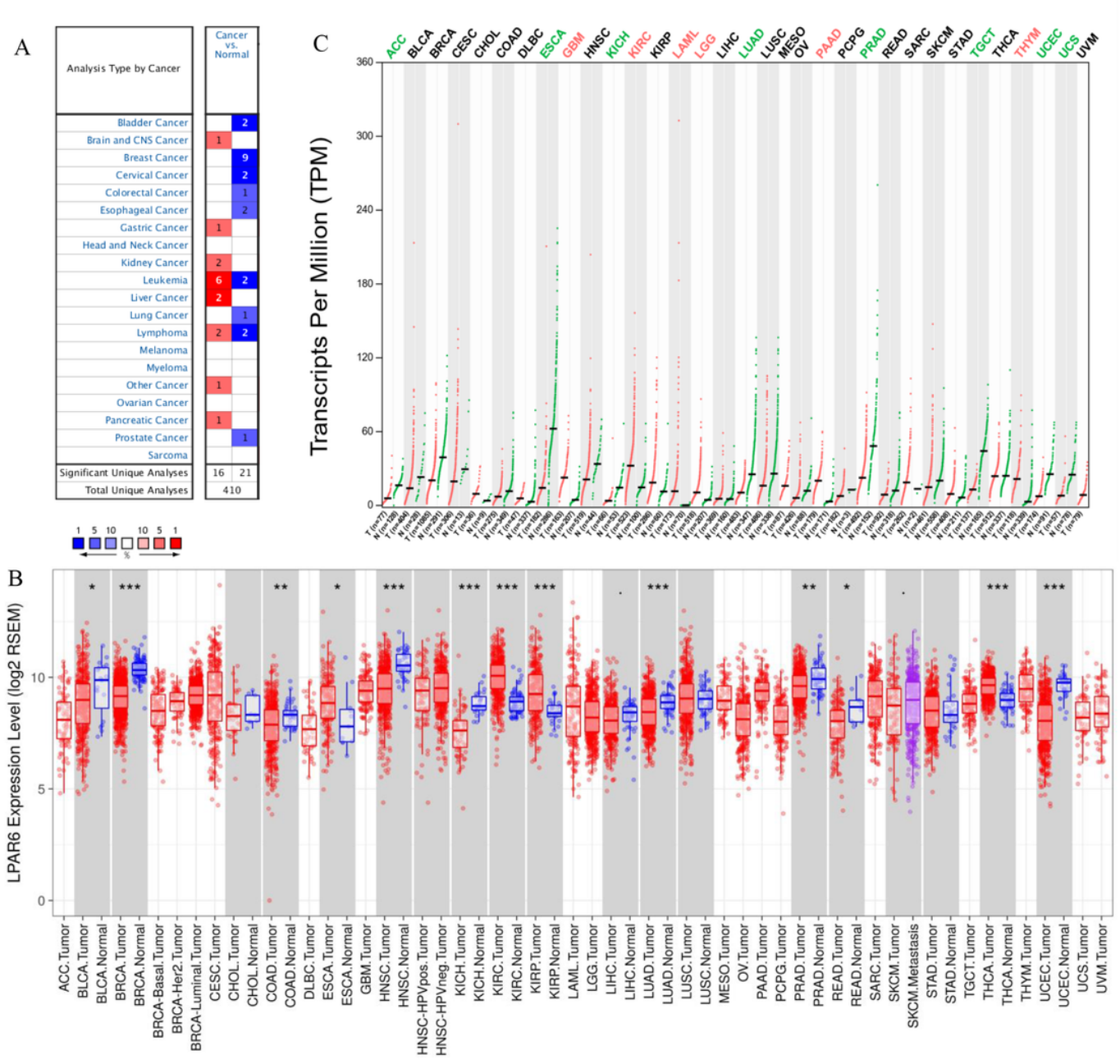

Figure 1

LPAR6 mRNA expression levels in different types of human cancers in different databases. (A) Increased or decreased LPAR6 in data sets of different cancers compared with normal tissues. Cell color is determined by the best gene rank percentile for the analyses within the cell. (B) Human LPAR6 expression levels in different tumor types from TCGA database. One category of cancer is in one box, and paired tissue (tumor and adjacent) are in grey boxes. . p<0.1, * p<0.05, **p<0.01, ***p<0.001. (C) LPAR6 expression profile across all tumor samples and paired normal tissues (Dot plot) via GEPIA. Each dots represent the expression of samples.

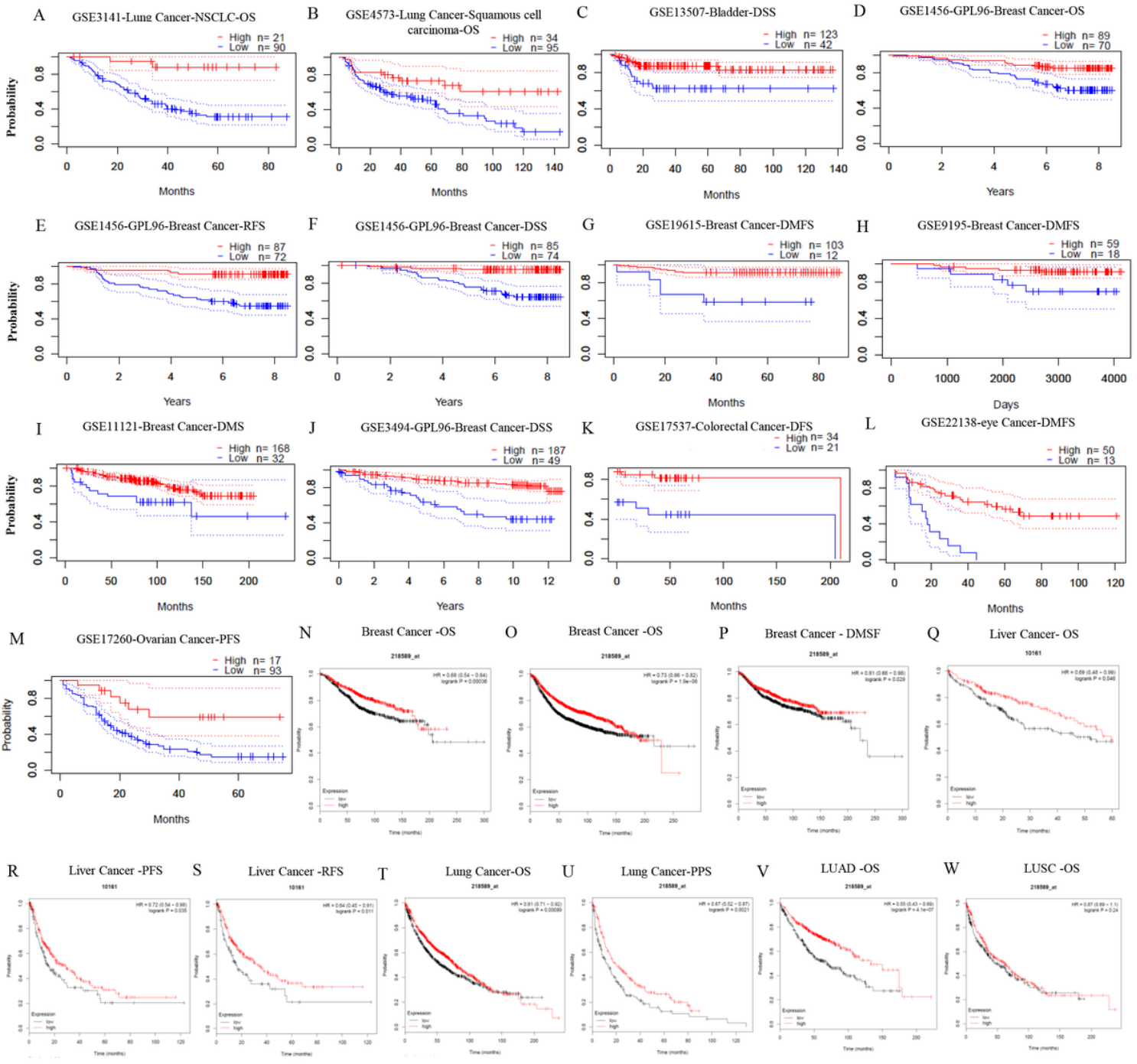

Figure 2

Kaplan-Meier survival curves comparing the high and low expression of LPAR6 in different types of cancer in the PrognoScan (A–M) and Kaplan-Meier plotter databases (N–W). (A-C) Survival curves of OS in two lung cancer cohorts [GSE3141 (n =111, P = 0.00206181) and GSE4573 (n =129 , P = 0.0219869)] and DSS in bladder cancer cohort [GSE13507 (n =165, P = 0.0067285)]. (D-F) Survival curves of OS, RFS and DFS in the breast cancer cohort [GSE1456-GPL96 (n =159, P = 0.00575883; P= 0.0000252; P= 0.000210173)]. (G-I) Survival curves of DMFS in the breast cancer cohort [GSE19615 (n=159, P = 0.00575883), GSE9195 (n=159, P = 0.0466683), GSE11121 (n=200 , P =0.0389008)]. (J-L) Survival curves of DSS in the breast, DFS in the colorectal and DMFS in the eye cancer cohort [GSE3494 (n=236, P = 0.00294205), GSE17537 (n=55, P = 0.0257972), GSE22138 (n=63, P = 0.00092478)]. (M) Survival curves of PFS in the ovarian cancer cohort [GSE17260 (n=110, P = 0.0392865)]. (N-P) Survival curves of OS (n =1402), RFS (n=3951) and DMSF (n=1746) in the breast cancer cohorts. (Q-S) Survival curves of OS (n=364), FPS (n=370) and RFS (n=316) in the liver cancer cohort. (T, U) Survival curves of OS (n=1926) and PPS (n=344) of the lung cancer. (V,W) Survival curves of OS of the lung adenocarcinoma (n=720) and squamous cell carcinoma (n=524).

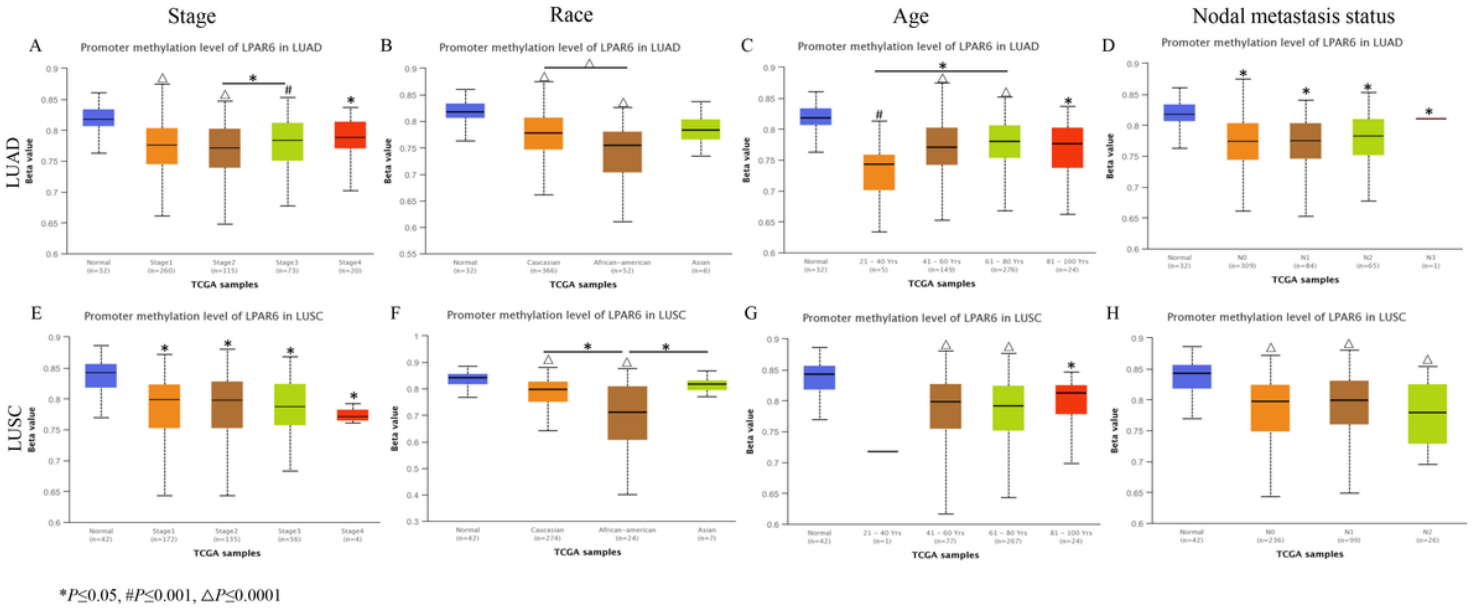

Figure 3

Promoter methylation levels of LPAR6 impacts the clinicopathological parameters in LUAD and LUSC cohorts. FIGURE 4 | Biological interaction network of LPAR6. LPAR6 interaction network in TCGA, different colors represent diverse bioinformatics methods (A) and differentially expressed genes in correlation with LPAR6 and heat maps of positively and negatively correlated genes with LPAR6 in LUAD and LUSC were analyzed by Pearson test (B). Red indicates positive and blue indicates negative.

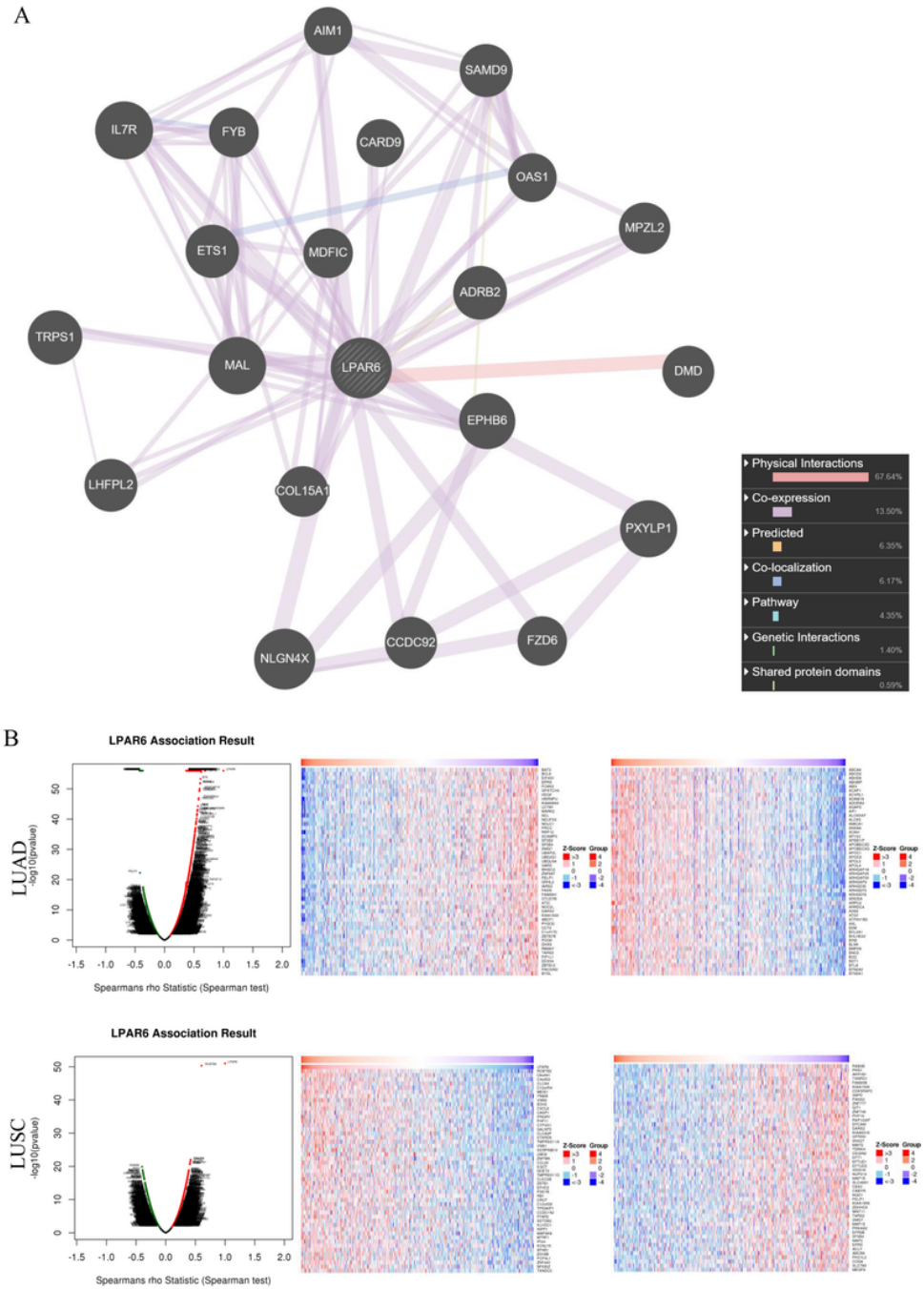

Figure 4

Biological interaction network of LPAR6. LPAR6 interaction network in TCGA, different colors represent diverse bioinformatics methods (A) and differentially expressed genes in correlation with LPAR6 and heat maps of positively and negatively correlated genes with LPAR6 in LUAD and LUSC were analyzed by Pearson test (B). Red indicates positive and blue indicates negative.

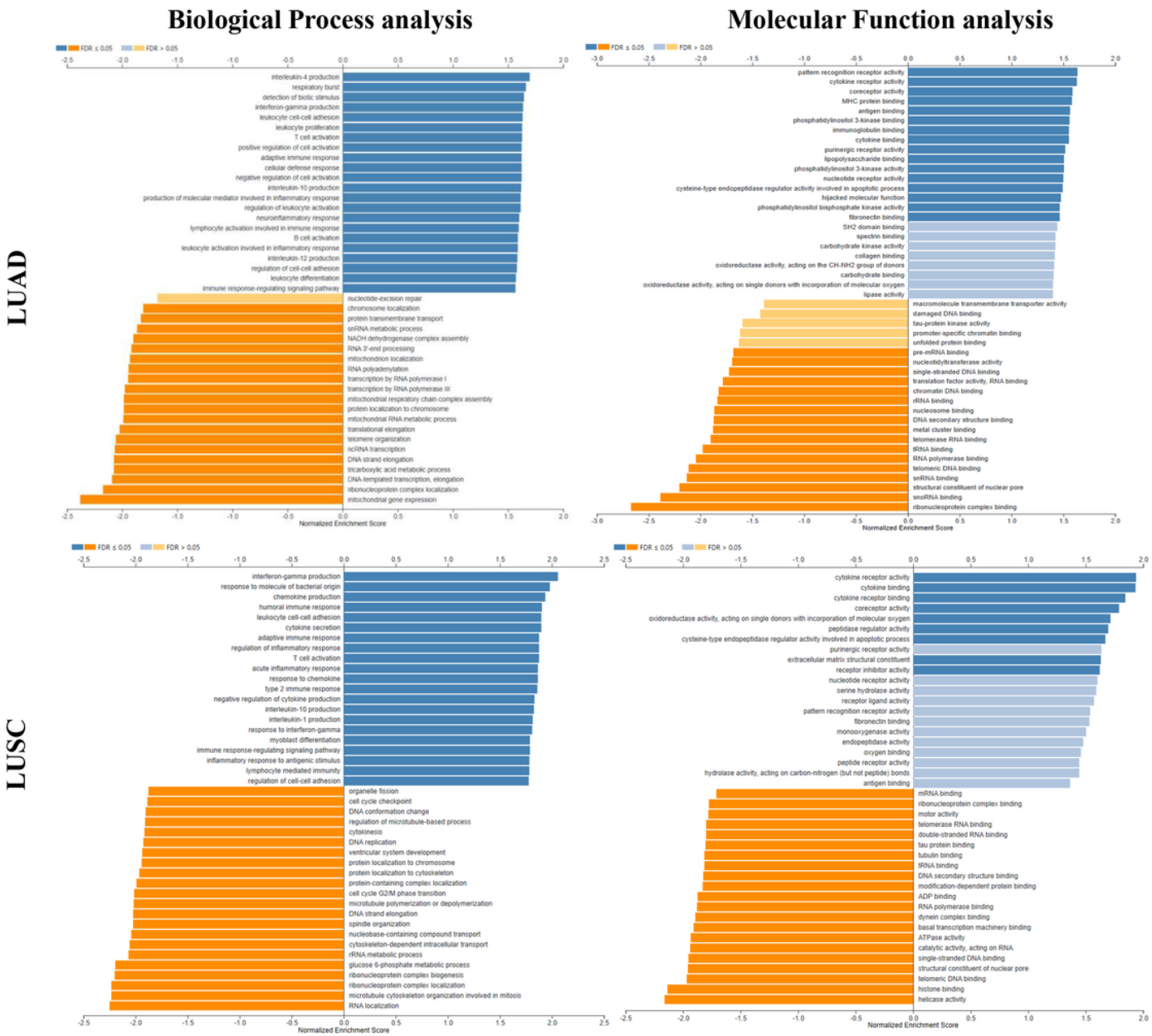

Figure 5

Enriched gene ontology annotations of biological process and molecular function analysis of LPAR6 correlated genes in LUAD (A), LUSC (B). Dark blue and orange indicate FDR≤0.05, light blue and orange indicate FDR >0.05. FDR, false discovery rate.

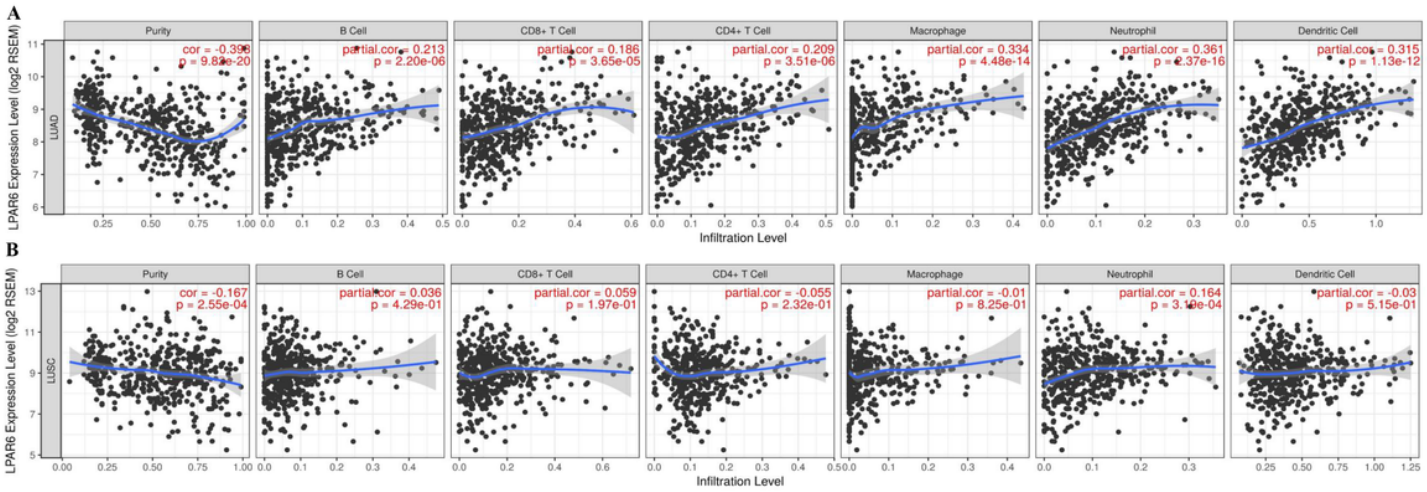

Figure 6

Correlation of LPAR6 expression with immune infiltration level in (A) LUAD, (B) LUSC. (A) LPAR6 expression is significantly negatively related to tumor purity and has significant strong positive correlations with the level of B cells, CD8+ T cells, macrophages, neutrophils, and DCs in LUAD (n = 515). (B) LPAR6 expression is significantly negatively related to tumor purity and has weak positive correlations with infiltrating levels of neutrophils in LUSC but no significant correlation with infiltrating levels of B cells, CD8+ T cells, macrophages and DCs (n = 501).

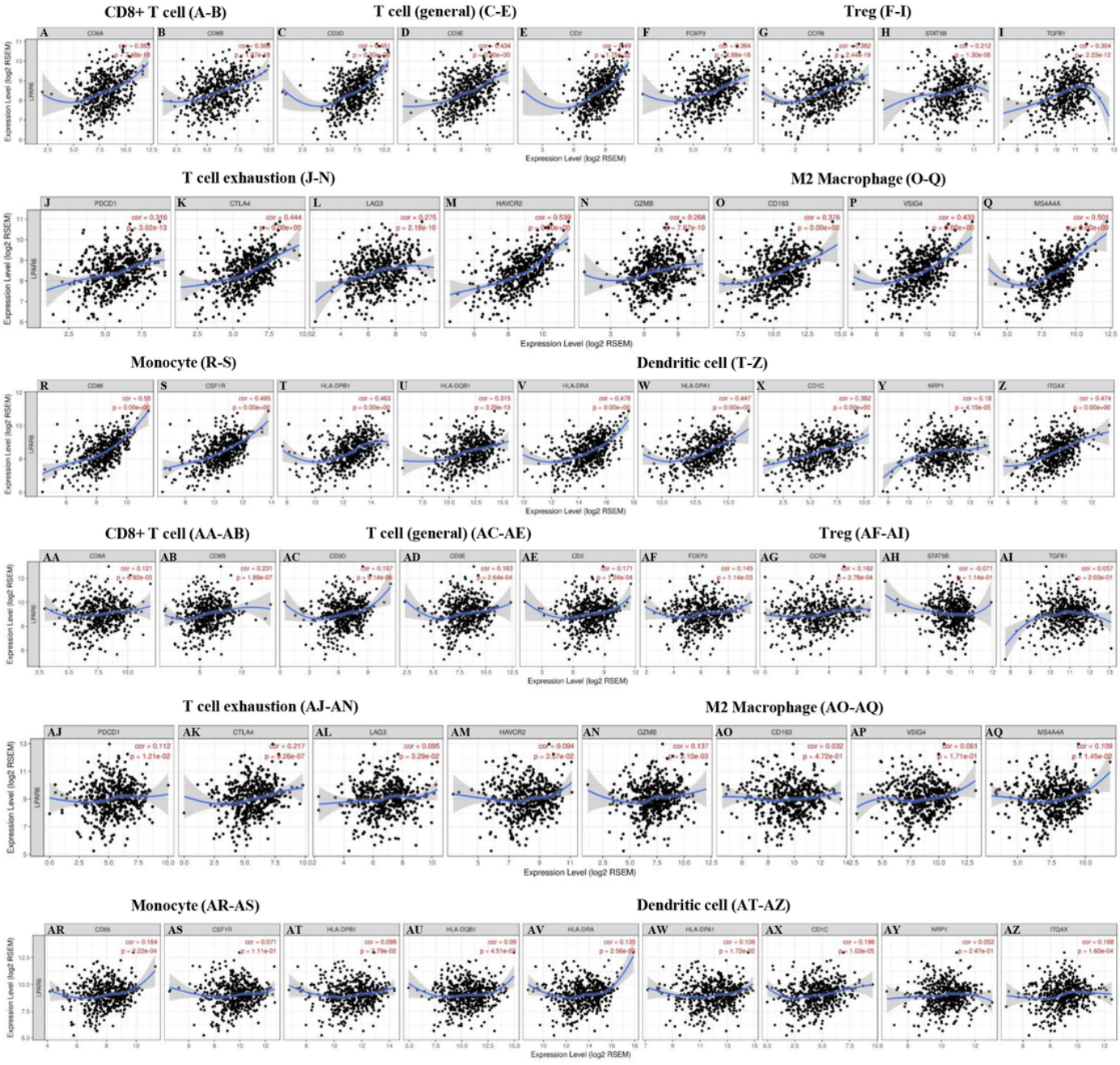

Figure 7

Correlation Analysis Between LPAR6 Expression and Immune Marker Sets in LUAD and LUSC. Markers include CD8A and CD8B of CD8+ T cell; CD3D, CD3E and CD2 of general T cell; FOXP3, CCR8, STAT5B and TGFB1 of Treg; PDCD1, CTLA4, LAG3, HAVCR2 and GZMB of exhausted T cells; CD163, VSIG4 and MS4A4A of M2 macrophages; CD86 and CSF1R of monocytes; HLA-DPB1, HLA-DQB1, HLA-DRA, HLA-DPA1, CD1C, NRP1 and ITGAX of Dendritic cell. (A–Z) Scatterplots of correlations between LPAR6 expression and gene markers of CD8+ T cell (A, B), general T cell (C-E), Treg (F-I), T cell exhaustion (J-N), M2 macrophage (O-Q), monocyte (R-S) and dendritic cell (T-Z) in LUAD. (AA–AZ) Scatterplots of correlations between LPAR6 expression and gene markers of CD8+ T cell (AA, AB), general T cell (AC-AE), Treg (AF-AI), T cell exhaustion (AJ-AN), M2 macrophage (AO-AQ), monocyte (AR-AS) and dendritic cell (AT-AZ) in LUSC.

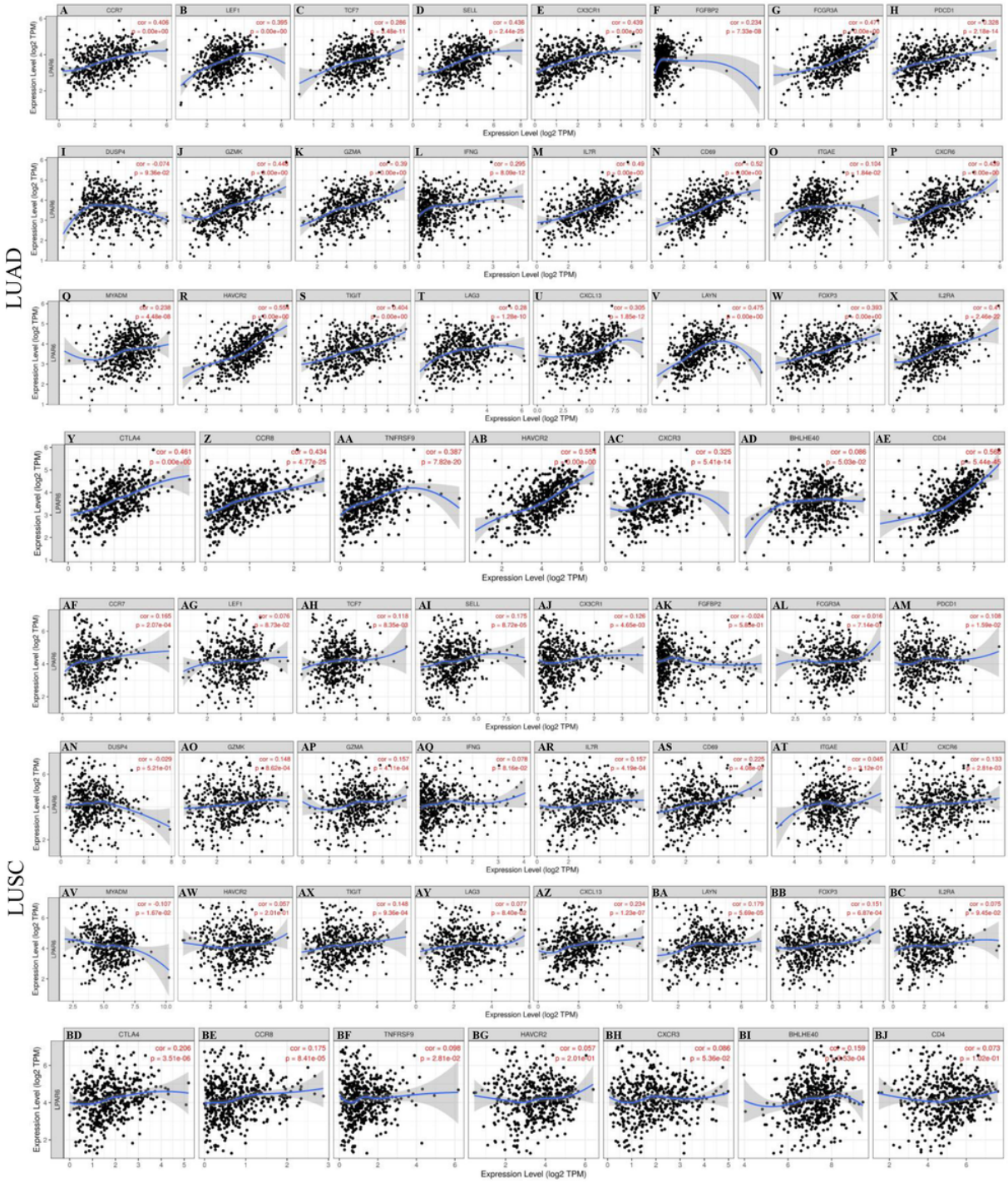

Figure 8

Correlation Analysis Between LPAR6 Expression and various T cell Marker Sets in LUAD and LUSC. (A–AE) Scatterplots of correlations between LPAR6 expression and gene markers of Naive T-Cell (CCR7, LEF1, TCF7, SELL) (A-D), Effector T-Cell (CX3CR1, FGFBP2, FCGR3A) (E-G), Effector memory T-Cell (PDCD1, DUSP4, GZMK, GZMA, IFNG) (H-L), Central memory T-Cell (CCR7, SELL, IL7R) (A, D, M), Resident memory T-Cell (CD69, ITGAE, CXCR6, MYADM) (N-Q), T cell exhaustion (HAVCR2, TIGIT, LAG3, PDCD1, CXCL13, LAYN) (R-T, H, U-V), Resting Treg (FOXP3, IL2RA) (W, X), Effector Treg (FOXP3, CTLA4, CCR8, TNFRSF9) (W, Y-AA), Th1-like (HAVCR2, IFNG, CXCR3, BHLHE40, CD4) (AB, L, AC-AE) in LUAD; (AF–BJ) Scatterplots of correlations between LPAR6 expression

and gene markers of Naive T-Cell (CCR7, LEF1, TCF7, SELL) (AF-AI), Effector T-Cell (CX3CR1, FGFBP2, FCGR3A) (AJ-AL), Effector memory T-Cell (PDCD1, DUSP4, GZMK, GZMA, IFNG) (AM-AQ), Central memory T-Cell (CCR7, SELL, IL7R) (AF, AI, AR), Resident memory T-Cell (CD69, ITGAE, CXCR6, MYADM) (AS-AV), T cell exhaustion (HAVCR2, TIGIT, LAG3, PDCD1, CXCL13, LAYN) (AW-AY, AM, AZ-BA), Resting Treg (FOXP3, IL2RA) (BB-BC), Effector Treg (FOXP3, CTLA4, CCR8, TNFRSF9) (BB, BD, BE-BF), Th1-like (HAVCR2, IFNG, CXCR3, BHLHE40, CD4) (BG, AQ, BI-BJ) in LUSC.

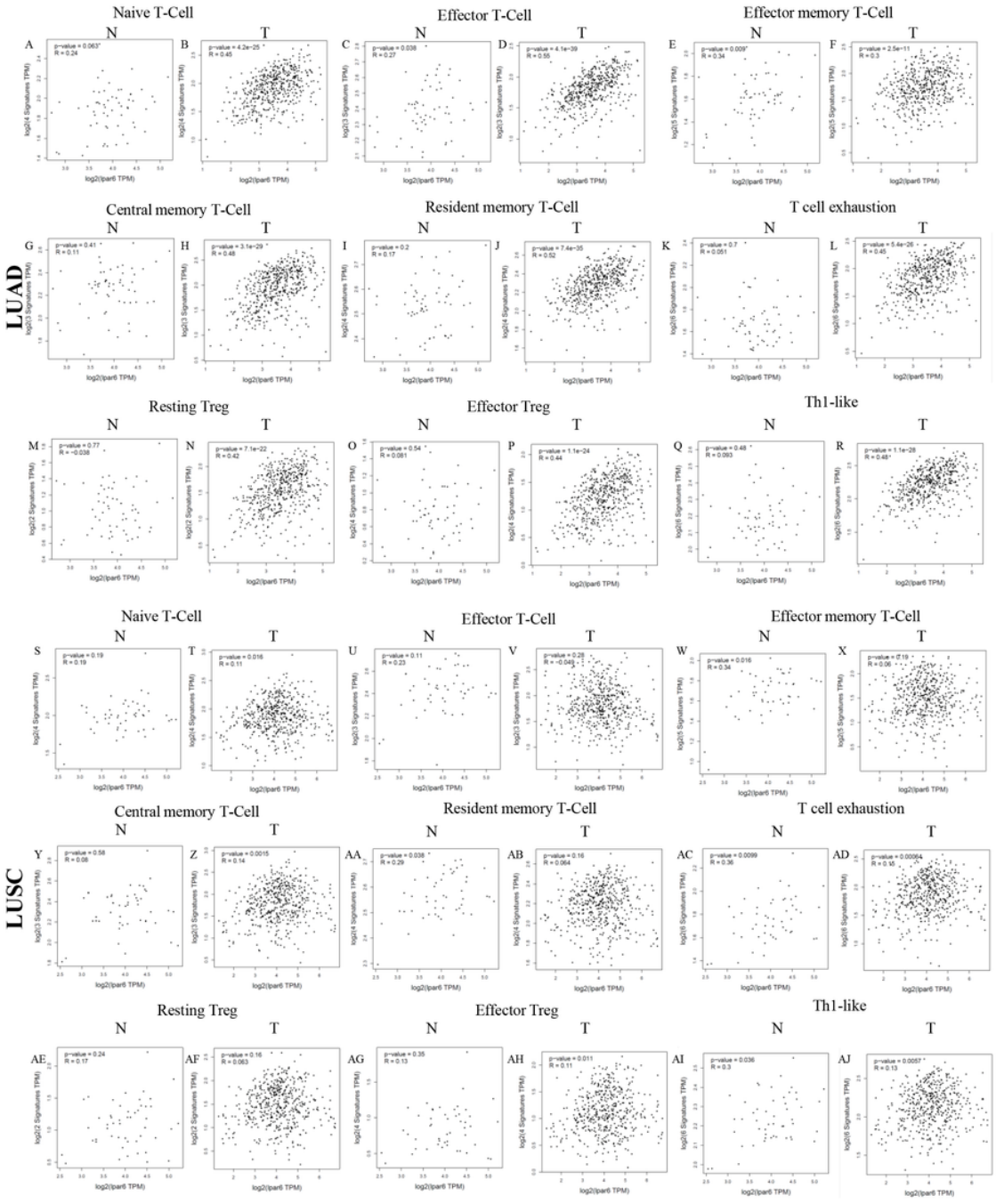

Figure 9

Correlation analysis between LPAR6 expression and various immune cells in normal and tumor tissue of LUAD and LUSC. (A–R) Scatterplots of correlations between LPAR6 expression and naive T-cell (A, B), effector T-cell (C, D), effector memory T-cell (E, F), central memory T-cell (G, H), resident memory T-cell (I, J), T cell exhaustion (K, L), resting Treg (M, N), effector Treg (O, P), Th1-like (Q, R) in the normal and tissue of LUAD; (S–AJ) Scatterplots of correlations between LPAR6 expression and gene markers of naive T-cell (S, T), effector T-cell (U, V), effector memory T-cell (W, X), central memory T-cell (Y, Z), resident memory T-cell (AA, AB), T cell exhaustion (AC, AD), resting Treg (AE, AF), effector Treg (AG, AH), Th1-like (AI-AJ) in LUSC.

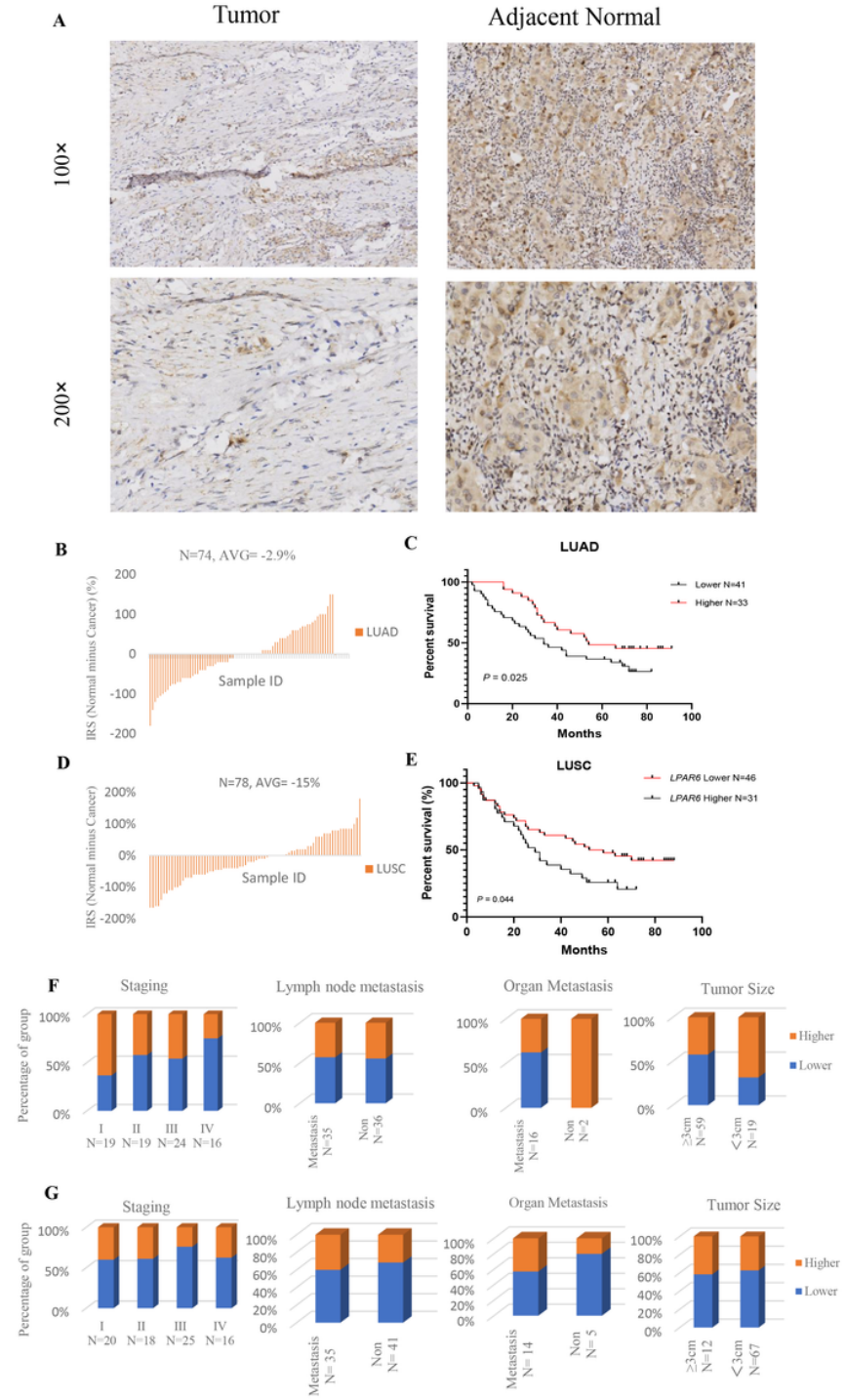

Figure 10

Higher expression of LPAR6 was correlated with clinicopathological parameters in LUAD cohort and was associated with increased overall survival (OS) of LUAD and LUSC patients. (A) Immunohistochemistry staining of the LPAR6 in the tumor and adjacent normal tissues. Red arrows indicated the cytoplasm-stained LPAR6. Bar, 50 μm; (B) The immunoreactive score (IRS) of the cytoplasm LPAR6 staining in 74 paired lung cancer tissues in LUAD cohort; (C) The Kaplan–Meier plot of the OS for lung cancer patients with relatively higher or lower LPAR6 expression levels in LUAD cohort (N = 74; Log-rank test, P =0.02); (D) The IRS of the cytoplasm LPAR6 staining in 78 paired lung cancer tissues in LUSC cohort; (E) The Kaplan–Meier plot of the overall survival for lung cancer patients with relatively higher or lower LPAR6 expression levels in LUSC cohort (N = 78; log-rank test, P =0.04). (F) The proportion of LPAR6 expression level (higher or lower) in different clinical stages, lymph node metastasis, organ metastasis and tumor size of patients in LUAD and LUSC cohorts.

Supplementary Files

This is a list of supplementary files associated with this preprint. Click to download.

- SIFig1.pdf
- SIFig2.pdf
- SITable1.docx
- SITable2.xlsx
- SITable3.docx
- SITable4.docx